

AFRL-AFOSR-UK-TR-2013-0032



**Inkjet assisted creation of self-healing layers between
composite plies**

**Professor Alma Hodzic
Dr. Patrick Smith**

**University of Sheffield
Advanced Manufacturing Research Centre and Composite Systems
Innovation Centre
Firth Ct
Sheffield, S10 2TP, United Kingdom**

EOARD Grant 11-3072

Report Date: July 2013

Final Report from 1 October 2011 to 30 September 2012

Distribution Statement A: Approved for public release distribution is unlimited.

**Air Force Research Laboratory
Air Force Office of Scientific Research
European Office of Aerospace Research and Development
Unit 4515 Box 14, APO AE 09421**

REPORT DOCUMENTATION PAGE

Form Approved OMB No. 0704-0188

Public reporting burden for this collection of information is estimated to average 1 hour per response, including the time for reviewing instructions, searching existing data sources, gathering and maintaining the data needed, and completing and reviewing the collection of information. Send comments regarding this burden estimate or any other aspect of this collection of information, including suggestions for reducing the burden, to Department of Defense, Washington Headquarters Services, Directorate for Information Operations and Reports (0704-0188), 1215 Jefferson Davis Highway, Suite 1204, Arlington, VA 22202-4302. Respondents should be aware that notwithstanding any other provision of law, no person shall be subject to any penalty for failing to comply with a collection of information if it does not display a currently valid OMB control number.
PLEASE DO NOT RETURN YOUR FORM TO THE ABOVE ADDRESS.

1. REPORT DATE (DD-MM-YYYY) 29 July 2013	2. REPORT TYPE Final Report	3. DATES COVERED (From – To) 1 October 2011 – 30 September 2012
--	---------------------------------------	---

4. TITLE AND SUBTITLE Inkjet assisted creation of self-healing layers between composite plies	5a. CONTRACT NUMBER FA8655-11-1-3072
	5b. GRANT NUMBER Grant 11-3072
	5c. PROGRAM ELEMENT NUMBER 61102F

6. AUTHOR(S) Professor Alma Hodzic Dr. Patrick Smith	5d. PROJECT NUMBER
	5d. TASK NUMBER
	5e. WORK UNIT NUMBER

7. PERFORMING ORGANIZATION NAME(S) AND ADDRESS(ES) University of Sheffield Advanced Manufacturing Research Centre and Composite Systems Innovation Centre Firth Ct Sheffield, S10 2TP, United Kingdom	8. PERFORMING ORGANIZATION REPORT NUMBER N/A
---	--

9. SPONSORING/MONITORING AGENCY NAME(S) AND ADDRESS(ES) EOARD Unit 4515 BOX 14 APO AE 09421	10. SPONSOR/MONITOR'S ACRONYM(S) AFRL/AFOSR/IOE (EOARD)
	11. SPONSOR/MONITOR'S REPORT NUMBER(S) AFRL-AFOSR-UK-TR-2013-0032

12. DISTRIBUTION/AVAILABILITY STATEMENT
Distribution A: Approved for public release; distribution is unlimited.

13. SUPPLEMENTARY NOTES

14. ABSTRACT
This project aimed to design and optimize a novel composite system using self-healing agent deposited in microscopically-ordered arrays through ink-jet printing, to arrest cracks along interfaces between composite plies. Novel aspects included the method itself, the highly-controlled crack arrest mechanism provided by self-healing microdroplets between plies, and the ability to rapidly transfer this technology into a prepreg manufacturing process. The approach consisted of depositing novel thermoplastic low-viscosity microdroplets with chemically and mechanically comparable properties to epoxy matrix in aerospace grade composites onto fiber-reinforced epoxy prepregs before curing using an ink-jet system. The report focuses on the most successful configuration using poly(methyl methacrylate) (PMMA) on Boeing-accredited toughened carbon fiber epoxy prepreg Cycom977-2. Double cantilever beam (DCB) and short beam shear (SBS) tests were used to evaluate the self-healing efficiency. It was shown that carefully selected printed self-healing agents increased both shear modulus and fracture toughness simultaneously, without imparting any parasitic weight, and restored the properties of the damaged and self-healed composite to a large degree following post-damage heat treatment. A patent application has been submitted by the University of Sheffield.

15. SUBJECT TERMS
EOARD, self-healing, crack arrest, composite manufacturing

16. SECURITY CLASSIFICATION OF:			17. LIMITATION OF ABSTRACT SAR	18. NUMBER OF PAGES 12	19a. NAME OF RESPONSIBLE PERSON Randall Pollak, Lt Col, USAF
a. REPORT UNCLAS	b. ABSTRACT UNCLAS	c. THIS PAGE UNCLAS			19b. TELEPHONE NUMBER (Include area code) +44 (0)1895 616115 DSN 314-235-6115



The University
Of
Sheffield.



Advanced Manufacturing Research Centre



CATAPULT
High Value Manufacturing



Composite
Systems
Innovation
Centre

Inkjet assisted creation of self-healing layers between composite plies

EOARD Award No: FA8655-11-1-3072

Professor Alma Hodzic and Dr Patrick Smith

Advanced Manufacturing Research Centre and Composite Systems Innovation Centre, The University of
Sheffield, United Kingdom

PI: Professor Alma Hodzic, AMRC, The University of Sheffield, UK

Research team at The University of Sheffield

Advanced Manufacturing Research Centre: Professor Alma Hodzic and Richard Grainger

Department of Mechanical Engineering: Dr Patrick Smith, Yi Zhang and Dr Jonathan Stringer

Department of Materials Science and Engineering: Elliot Fleet

Period of performance: 01 October 2011 – 30 September 2012

Table of Contents

1. Summary
2. Methods, Assumptions and Procedures
 - 2.1. Inkjet printed composites manufacturing
 - 2.2. Optical Microscopy
 - 2.3. Mechanical tests and results
3. Conclusions
4. Acknowledgements

List of Figures

Fig.1. Hexagonal printed pattern of self-healing agent in composites.

Fig. 2.2.1 Optical images of PMMA dots with fluorescein on glass slides under different conditions: (a) before curing cycle, (b) after heating to 100° C and (c) after the complete curing cycle.

Fig. 2.2.2 Optical images of PMMA dots with fluorescein on CFRP prepreg under different conditions: (a) before curing cycle, (b) after heating to 100° C and (c) after the complete curing cycle.

Fig. 2.2.3 Fluorescein images of PEG dots on pre-preg under different conditions: (a) before curing cycle, (b) after heating to 50° C and (c) after the complete curing cycle.

Fig. 2.2.4 Fluorescein images of PMMA dots on pre-preg under different conditions: (a) before curing cycle, (b) after heating to 100° C and (c) after the complete curing cycle.

Fig.2.2.5. Interferometry images of PMMA dots on glass slides under different conditions: (a) before curing, (b) after curing.

Fig.2.2.6. Interferometry images of PMMA dots on prepreg under different conditions: (a) before curing, (b) after curing.

Fig. 2.3.1 Load-displacement curve for a DCB Mode I test showing initiation from the resulting mode I precrack followed by crack propagation and unloading.

Fig. 2.3.2 G_{IC} comparisons for NL point, 5% / MAX point and avg. PROP point before and after healing cycle. The connector line shows a large degree of the recovered portion (self-healing efficiency) of the original propagation G_{IC} value (printed PMMA sample compared to the unprinted virgin sample after damage and self-healing).



The
University
Of
Sheffield.



Advanced Manufacturing Research Centre



CATAPULT
High Value Manufacturing



Composite
Systems
Innovation
Centre

List of Tables

Table 2.1 Inkjet-Printing parameters used in this study.

Table 2.3.1 SSB method testing schema.

Table 2.3.2. SBS results for test group *i*: No induced damage and no healing cycle.

Table 2.3.3. SBS results for test group *ii*: No induced damage with the healing cycle.

Table 2.3.4. SBS results for test group *iii*: damaged and no healing cycle.

Table 2.3.5. SBS results for test group *iv*: both damaged and healed specimens.

Table 2.3.6. Summary of SBS test results.

1. Summary

This project aimed to design and optimise a novel self-healing (SH) advanced composite system using minimum SH agent (~0.02%), deposited in microscopically ordered arrays through ink-jet printing, to arrest cracks along interfaces between plies as shown in Fig.1. Novel aspects included the method itself, the highly-controlled crack arrest mechanism provided by SH microdroplets between plies, and the ability to rapidly transfer this new technology into a prepreg manufacturing process. Results identified the optimum size and spacing of microdroplets capable for crack arrest in multi-axial directions

between plies, as well as desired manufacturing method and speed of deposition. The approach consisted of depositing novel thermoplastic low-viscosity microdroplets with chemically and mechanically comparable properties to epoxy matrix in aerospace grade composites onto fibre reinforced epoxy prepreps before curing. The SH agents remained arrested and encapsulated between epoxy plies without direct contact with neighboring microdroplets. This ensured consistent integrity of the composite while preserving SH capability. In addition, the spatial control offered by ink-jet printing with the four-fluid printhead assembly at The University of Sheffield allowed optional study of compositional variation in SH agents to optimise SH efficiency. In addition, a comparison was made between the systems with discretely printed SH agents and fully covered plies using the same printing method. The efficiency of discrete (hexagonal) patterns was higher compared to the fully printed surfaces, as the former method enabled the adjacent composite plies to cure without the loss in chemical adhesion.

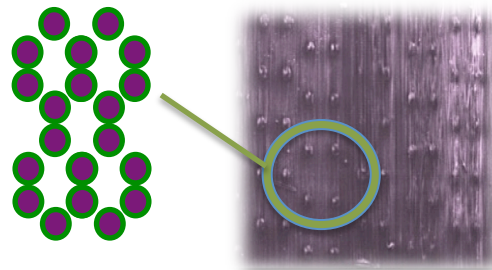


Fig.1. Hexagonal printed pattern of self-healing agent in composites.

The focus of this technical report is to present the most successful results obtained by printing poly(methyl methacrylate) (PMMA) using Boeing accredited toughened carbon fibre epoxy prepreg Cycom977-2 as the substrate. In order to investigate the self-healing efficiency, damage process was employed to introduce appropriate amount of damage into specimens to demonstrate self-healing. Double cantilever beam (DCB) and short beam shear (SBS) tests have been adopted to evaluate the self-healing efficiency.

It was shown that carefully selected printed self-healing agents increased both shear modulus and fracture toughness of CFRP simultaneously, and without imparting any parasitic weight, restored the properties of the damaged and self-healed composite to a large degree, following the post-damage heat treatment. The specimens with printed PMMA exhibited the highest mode I interlaminar fracture toughness (G_{IC}) and the shear modulus both before and after healing cycles among the studied groups. The imparted toughening, stiffening and self-healing properties through the method of PMMA discrete deposition at only ~0.02% weight fraction represent a successful achievement from the project that was initially based on a high-risk idea that has not been attempted before. The results presented in this report were recently submitted to UK Patent Office by The University of Sheffield under Patent No. 1312551.3.

2. Methods, Assumptions and Procedures

Experimental work consisted of identifying the optimal parameters for accurate deposition of inkjet printed polymers, suitable thermoplastic self-healing agents for high-temperature CFRP, and selection of mechanical tests appropriate for inter-ply structural investigation involving a complex matrix of specimens both without and with printed SH agents.

2.1 Inkjet printed composites manufacturing

Piezoelectric inkjet printers can accurately deposit pico-litre volumes of solutions or suspensions in well-defined patterns. The materials and parameters defining the inkjet printing of polymers used in this work are presented in Table 1.

Table 2.1 Inkjet-Printing parameters used in this study.

Group	Composition of ink			Diameter of printhead / μm	Pattern	Substrate
	Solute	wt %	Solvent			
PMMA	PMMA	5	DMF*	60	Hexagon	977-2
PEG+Water	PEG	5	Distilled water	60	Hexagon	977-2
PEG+Ethanol	PEG	5	Pure Ethanol	60	Hexagon	977-2

$M_n(\text{PMMA}) = 15,000$; $M_n(\text{PEG}) = 20,000$; DMF*: N,N-Dimethylformamide

Following the deposition of inkjet printed patterns, the composites were cured and manufactured following the recommended thermal cycle:

Curing cycle for Cycom977-2 pre-preg

- ① Ramp: $20^\circ\text{C} \rightarrow 100^\circ\text{C}$ (rate: $2^\circ\text{C} / \text{min}$)
- ② Dwell: 30min
- ③ Ramp: $100^\circ\text{C} \rightarrow 177^\circ\text{C}$ (rate: $2^\circ\text{C} / \text{min}$)
- ④ Dwell: 120min
- ⑤ Ramp: $177^\circ\text{C} \rightarrow 20^\circ\text{C}$ (rate: $2^\circ\text{C} / \text{min}$)

Damage process was carried out using a tensometer to perform SBS test, to induce the ‘equivalent’ amount of damage to all specimens, and the healing cycle imitated the curing cycle in order to investigate the harshest temperature environment that the composite may be subjected to at this stage.

2.2 Optical microscopy

OM was used (CK40-SLP, OLYMPUS) to investigate the behaviour of PMMA dots printed on glass slide, as shown in Figure 2.2.1, during the various stages of thermal cycle.

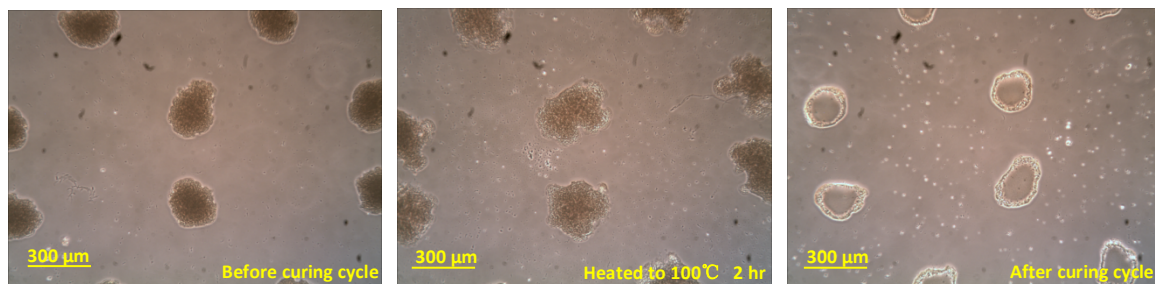


Fig. 2.2.1 Optical images of PMMA dots with fluorescein on glass slides under different conditions: (a) before curing

cycle, (b) after heating to 100° C and (c) after the complete curing cycle.

Coffee staining effect was evident after the full cure cycle was completed, however the droplets preserved their geometry and the surface aspect ratio. A similar investigation was carried out on the printed carbon fibre prepreg, as shown in Fig. 2.2.2. However in this case, the droplets of PMMA were not clearly observed following the curing cycle, indicating the reaction with epoxy during the curing process.

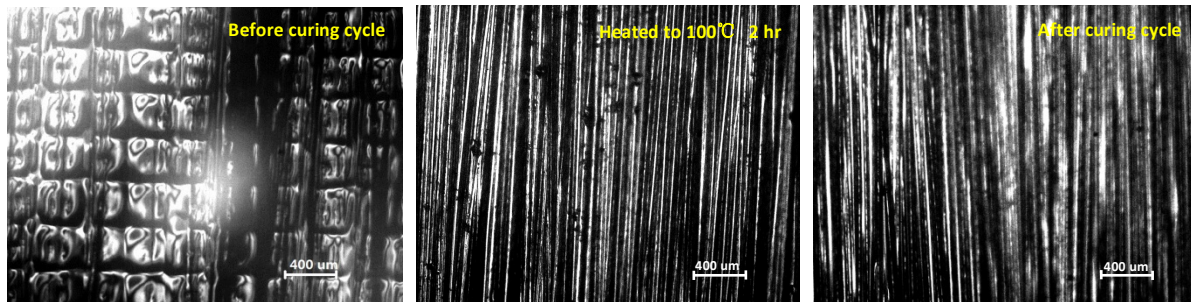


Fig. 2.2.2 Optical images of PMMA dots with fluorescein on CFRP prepreg under different conditions: (a) before curing cycle, (b) after heating to 100° C and (c) after the complete curing cycle.

In order to investigate this effect further, fluorescein was added to PMMA and PEG during the printing process to help identify the deposited droplets during the thermal cycle, as shown in Figs. 2.2.3 and 2.2.4.

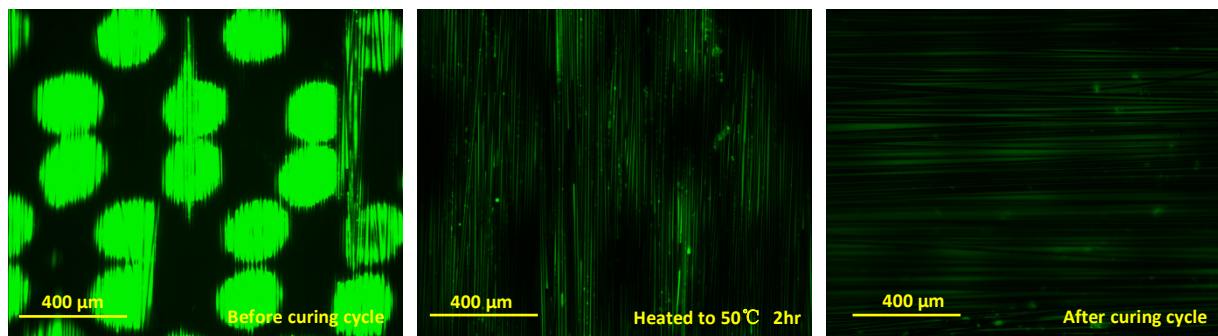


Fig. 2.2.3 Fluorescein images of PEG dots on pre-preg under different conditions: (a) before curing cycle, (b) after heating to 50° C and (c) after the complete curing cycle.

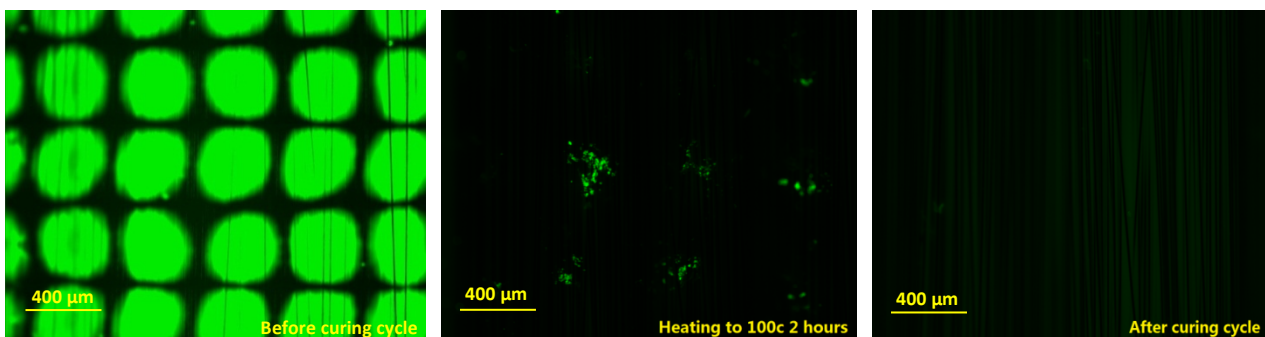


Fig. 2.2.4 Fluorescein images of PMMA dots on pre-preg under different conditions: (a) before curing cycle, (b) after heating to 100° C and (c) after the complete curing cycle.

From Figures 2.2.3 and 2.2.4, it can be seen that printed fluorescein within PEG and PMMA dots disappeared after heating. There could be two explanations: the polymer penetrated into the epoxy during the thermal cycle,

or the fluorescein itself reacted and evaporated during the process.

This part of investigation was finalised using Contour GT (Interferometer) to image PMMA droplets printed on glass slide and prepreg, as shown in Figs. 2.2.5 and 2.2.6 respectively.

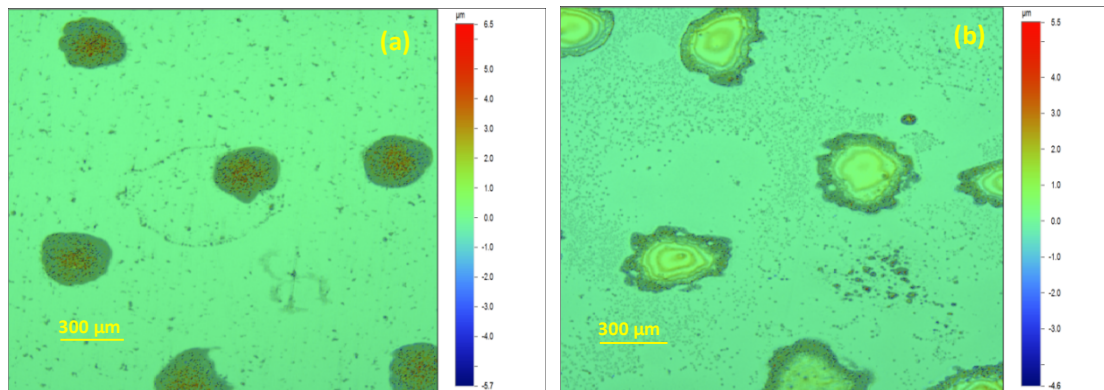


Fig.2.2.5. Interferometry images of PMMA dots on glass slides under different conditions: (a) before curing, (b) after curing.

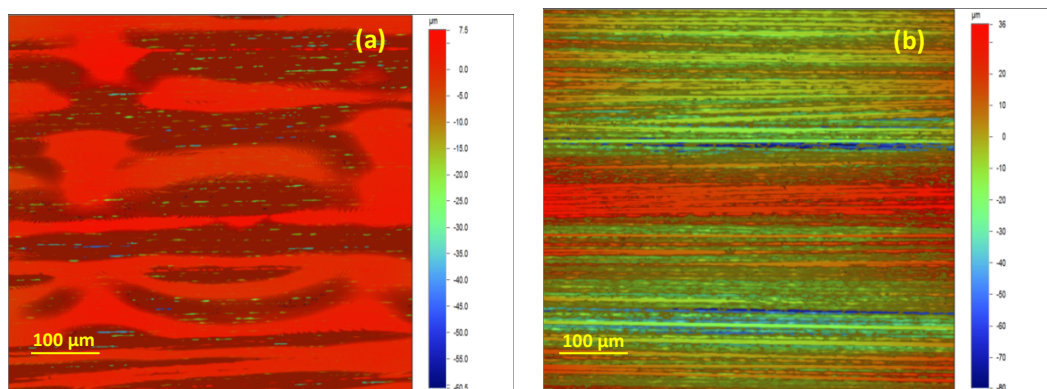


Fig.2.2.6. Interferometry images of PMMA dots on prepreg under different conditions: (a) before curing, (b) after curing.

The interferometry results suggested that the printed PMMA droplets reacted with the epoxy during the curing cycle, and their visibility was not as evident as on the glass slides. However, their distinct chemical composition guaranteed the preservation of thermoplastic ‘islands’ in the material after the heating process.

2.3 Mechanical Tests and Results

In this part of the study, two standard mechanical tests were used to evaluate the structural integrity and self-healing efficiency of the inkjet printed engineered composite material.

2.3.1 Fibre-reinforced plastic composites — Determination of apparent interlaminar shear strength by short-beam method. (BS EN ISO 14130:1998)

Table 2.3.1 SSB method testing schema.

	i	ii	iii	iv
Damaged	×	×	√	√
Healed	×	√	×	√

Each batch of test specimens was allocated one of the above four test groups. All specimens were used only once; ‘damaged’ group implied using SBS test to introduce the equivalent amount of damage across the group; ‘healed’ was used to label the group of test specimens subjected to the secondary curing (healing) cycle.

Table 2.3.2. SBS results for test group *i*: No induced damage and no healing cycle.

	Slope ($\times 10^3$ N/mm)		Maximum Load ($\times 10^3$ N)		τ_M (MPa)	
	Avg.	SD	Avg.	SD	Avg.	SD
Virgin	5.340	0.355	2.985	0.228	111.9	8.5
5%PEG+Ethanol	5.781	0.177	2.817	0.107	105.6	4.3
5%PEG+Water	7.093	0.239	3.590	0.105	134.6	3.9
5%PMMA+DMF	7.147	0.082	3.118	0.081	116.9	3.0

*SD: standard deviation

It can be seen that samples with printed self-healing agent possessed higher shear modulus, with printed PMMA samples showing the highest shear modulus, indicating a synergistic mechanism between the printed droplets and the base material. Further, there is no significant difference among the virgin and printed samples regarding to the average maximum load and the average maximum interlaminar shear strength, showing clearly that the structural integrity of the composite has been preserved with printed additives.

Table 2.3.3. SBS results for test group *ii*: No induced damage with the healing cycle.

	Slope ($\times 10^3$ N/mm)		Maximum Load ($\times 10^3$ N)		τ_M (MPa)	
	Avg.	SD	Avg.	SD	Avg.	SD
Virgin	5.900	0.368	3.170	0.269	118.9	10.1
5%PEG+Ethanol	6.780	0.044	3.088	0.128	115.8	4.8
5%PEG+Water	6.906	0.145	3.363	0.088	126.1	3.3
5%PMMA+DMF	7.205	0.406	3.177	0.066	119.1	2.5

It can be seen that the samples with printed SH agent possessed higher shear modulus than that of the virgin samples after the secondary heating cycle, again the highest stiffness associated with PMMA printed composites. Again, there is no significant difference between the virgin and self-healing agent printed samples regarding to the average maximum load and average maximum interlaminar shear stress values, indicating

that SH agents can impart beneficial properties throughout the service life of the composite.

Comparing groups i and ii, it can be seen that the average maximum interlaminar shear strength (τ_M), the average maximum load and the average shear modulus were slightly enhanced after the healing cycle, which could be either caused by the printed self-healing agent or by the post curing of epoxy in the prepreg itself, or both.

Table 2.3.4. SBS results for test group *iii*: damaged and no healing cycle.

	Slope ($\times 10^3$ N/mm)		Maximum Load ($\times 10^3$ N)		τ_M (MPa)	
	Avg.	SD	Avg.	SD	Avg.	SD
Virgin	4.268	0.172	2.463	0.079	92.4	3.0
5%PEG+Ethanol	5.620	0.283	2.376	0.235	89.1	8.8
5%PEG+Water	6.061	0.537	3.054	0.318	114.6	11.9
5%PMMA+DMF	5.770	0.393	2.593	0.073	97.3	2.7

We can see the mechanical properties of the four groups being reduced after the induced damage. The samples with the printed self-healing agent possessed higher shear modulus compared to the virgin samples. Further, no significant difference is observed regarding to the average maximum load and the average maximum interlaminar shear stress among the four groups, similar to the previous results. Since the same degree of damage process cannot be guaranteed in each test specimen, the results in some groups had a higher standard deviation.

Table 2.3.5. SBS results for test group *iv*: both damaged and healed specimens.

	Slope ($\times 10^3$ N/mm)		Maximum Load ($\times 10^3$ N)		τ_M (MPa)	
	Avg.	SD	Avg.	SD	Avg.	SD
Virgin	5.046	1.011	2.520	0.406	94.5	15.2
5%PEG+Ethanol	5.224	0.464	2.486	0.300	93.2	11.3
5%PEG+Water	6.334	0.502	2.881	0.339	108.1	12.7
5%PMMA+DMF	5.756	0.316	2.674	0.174	100.3	6.5

After the process of damage and self-healing, it can be seen that the samples with printed SH agents were slightly improved compared to the virgin systems. Considering that SBS experiments were conducted with the aim of evaluating the structural integrity of the material with printed SH agents, we conclude that the materials' properties and structural integrity have been successfully preserved and slightly enhanced both before and after self-healing cycle. In order to evaluate the SH efficiency, Mode I DCB (Double Cantilever Beam) test was performed and presented in the following sections.

Table 2.3.6. Summary of SBS test results.

	Damage	Heal	Average value n = 5					
			Slope ($\times 10^3$ N/mm)	SD*	Load _{MAX} ($\times 10^3$ N)	SD*	τ_M (MPa)	SD*
Virgin	×	×	5.340	0.355	2.985	0.228	111.9	8.5
	×	√	5.900	0.368	3.170	0.269	118.9	10.1
	√	×	4.268	0.172	2.463	0.079	92.4	3.0

	√	√	5.046	1.011	2.520	0.406	94.5	15.2
5%PEG + Water	×	×	7.093	0.239	3.590	0.105	134.6	3.9
	×	√	6.906	0.145	3.363	0.088	126.1	3.3
	√	×	6.061	0.537	3.054	0.318	114.6	11.9
	√	√	6.334	0.502	2.881	0.339	108.1	12.7
5%PEG + Ethanol	×	×	5.781	0.177	2.817	0.107	105.6	4.3
	×	√	6.780	0.044	3.088	0.127	115.8	4.8
	√	×	5.620	0.283	2.376	0.235	89.1	8.8
	√	√	5.224	0.464	2.486	0.300	93.2	11.3
5%PM MA + DMF	×	×	7.147	0.082	3.118	0.081	116.9	3.0
	×	√	7.205	0.406	3.177	0.066	119.1	2.5
	√	×	5.770	0.393	2.593	0.073	97.3	2.7
	√	√	5.756	0.316	2.674	0.174	100.3	6.5

2.3.2 Fibre-reinforced plastic composites — Determination of mode I interlaminar fracture toughness, G_{IC} , for unidirectionally reinforced materials. (BS ISO 15024:2001)

According to the standard, there are several important G_{IC} values of particular points as explained below:

- 1) **NL point** – the point of deviation from linearity on the load versus extension trace;
- 2) **5 % / MAX point** – the point which occurs first on the loading the specimen between:
 - a) The point of 5 % increase in compliance ($C_{5\%}$) from its initial value (C_0);
 - b) The maximum load point.
- 3) **PROP points** – points of discrete delamination length increments beyond the tip of the insert or starter crack tip marked on the load-extension trace, points where the crack has been arrested being excluded.

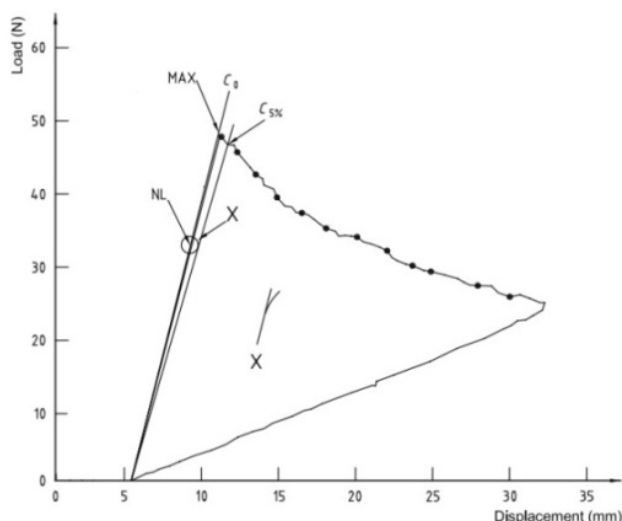


Fig. 2.3.1 Load-displacement curve for a DCB Mode I test showing initiation from the resulting mode I precrack followed by crack propagation and unloading.

2.3.2.1 DCB Mode I test results

The summary of all results is presented in Fig. 2.3.2 in the form of average values across all groups before and after damage and self-healing.

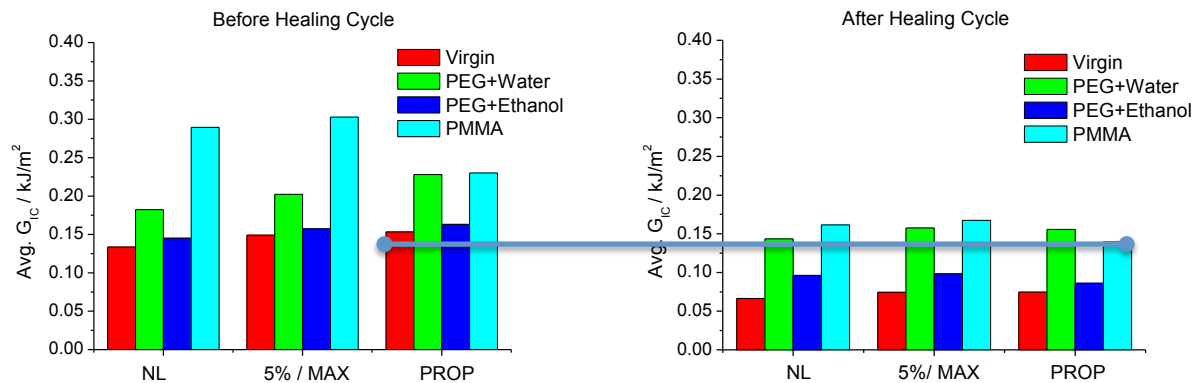


Fig. 2.3.2 G_{IC} comparisons for NL point, 5% / MAX point and avg. PROP point before and after healing cycle. The connector line shows a large degree of the recovered portion (self-healing efficiency) of the original propagation G_{IC} value (printed PMMA sample compared to the unprinted virgin sample after damage and self-healing).

From Figure 2.3.2, we can see the average G_{IC} values of NL, 5% / MAX and avg. PROP points of PMMA printed specimens are higher than that of the virgin and PEG printed specimens, both before and after healing cycles, indicating that the printed PMMA enhanced the interlaminar fracture toughness of specimens. The fracture toughness of the system was recovered almost to the virgin value with the assistance of discretely printed PMMA between the plies, as shown with the connecting line.

3. Conclusions

The fracture toughness results, obtained by the fully destructive DCB Mode I interlaminar test, showed approximately double values both before and after self-healing for the printed PMMA material in CFRP composites. As the indication of self-healing efficiency, when the value for PMMA printed system after the healing cycle is compared to the virgin material before the healing cycle, it can be seen that the original properties of the virgin material have been recovered to a large degree (~90%). Strong toughening and self-healing capability of the system was achieved due to the unique ability of the selected thermoplastic polymer to react with the epoxy resin in carbon fibre reinforced composites, and by enabling the discrete deposition of the SH agent, and thereby retaining (or enhancing) the composite's original structural properties. Considering that the composite system used in this study is already toughened and hardened to comply with the stringent requirements for aerospace composites, the imparted toughening, stiffening and self-healing properties through the method of PMMA discrete deposition at ~0.02% weight fraction represent a very successful achievement from the project that was initially based on a high-risk idea that has not been attempted before. Furthermore, the manufacturing of these composites can be automatically scaled up without causing any disruption to the existing composites supply chain, and without a need to develop new equipment.

4. Acknowledgements

Effort sponsored by the Air Force Office of Scientific Research, Air Force Material Command, USAF, under grant number FA8655-11-1-3072. The U.S. Government is authorised to reproduce and distribute reprints for Governmental purpose notwithstanding any copyright notation thereon. We also wish to thank our colleagues from EOARD and AFOSR for their encouragement and intellectual support.